Proteomic basis of modulation of post ischemic fibrosis by MSC exosomes

Article *in* AJP Regulatory Integrative and Comparative Physiology · August 2021

DOI: 10.1152/ajpregu.00124.2021

6 authors, including:

Raj Kore
University of Arkansas for Medical Sciences
32 PUBLICATIONS **348** CITATIONS
SEE PROFILE

Xianwei Wang
University of Arkansas for Medical Sciences
95 PUBLICATIONS **2,840** CITATIONS
SEE PROFILE

Jeffrey Curran Henson
University of Arkansas for Medical Sciences
13 PUBLICATIONS **41** CITATIONS
SEE PROFILE

Zufeng Ding
University of Arkansas for Medical Sciences
74 PUBLICATIONS **2,029** CITATIONS
SEE PROFILE

AMERICAN JOURNAL OF PHYSIOLOGY
REGULATORY, INTEGRATIVE AND COMPARATIVE PHYSIOLOGY

Am J Physiol Regul Integr Comp Physiol 321: R639–R654, 2021.
First published August 25, 2021; doi:10.1152/ajpregu.00124.2021

RESEARCH ARTICLE

Don't Deny Your Inner Environmental Physiologist: Investigating Physiology with Environmental Stimuli

Proteomic basis of modulation of postischemic fibrosis by MSC exosomes

Rajshekhar A. Kore,[1] Xianwei Wang,[2] Jeffrey Curran Henson,[1] Zufeng Ding,[1] Azemat Jamshidi-Parsian,[3] and Jawahar L. Mehta[1]

[1]*Cardiology Section, Central Arkansas Veterans Healthcare System, and the University of Arkansas for Medical Sciences, Little Rock, Arkansas;* [2]*Department of Pharmacology, Xinxiang Medical University, Xinxiang, China; and* [3]*Department of Radiation Oncology, University of Arkansas for Medical Sciences, Little Rock, Arkansas*

Abstract

After an ischemic event, there is activation of fibroblasts leading to scar formation. It is critical to limit the profibrotic remodeling and activate the reparative remodeling phase to limit cardiac diastolic dysfunction. Mesenchymal stem cell (MSC) exosomes offer significant protection against ischemia-related systolic dysfunction. Here, we studied if MSC exosomes would offer protection against profibrotic events in mouse hearts subjected to acute ischemia [1 h left coronary artery (LCA) occlusion] or chronic ischemia (7 days LCA occlusion). After acute ischemia, there was activation of inflammatory signals, more in the peri-infarct than in the infarct area, in the saline (vehicle)-treated mice. At the same time, there was expression of cardiac remodeling signals (vimentin, collagens-1 and -3, and fibronectin), more in the infarct area. Treatment with MSC exosomes before LCA ligation suppressed inflammatory signals during acute and chronic ischemia. Furthermore, exosome treatment promoted pro-reparative cardiac extracellular matrix (ECM) remodeling in both infarct and peri-infarct areas by suppressing fibronectin secretion and by modulating collagen secretion to reduce fibrotic scar formation through altered cellular signaling pathways. Proteomics study revealed intense expression of IL-1β and activation of profibrotic signals in the saline-treated hearts and their suppression in MSC exosome-treated hearts. To our knowledge, this is the first report on the infarct and peri-infarct area proteomics of ischemic mice hearts to explain MSC exosome-mediated suppression of scar formation in the ischemic mouse hearts.

collagens; cardiac fibrosis; heart proteomics; myocardial ischemia; stem cell exosomes

INTRODUCTION

In a normal heart, cardiac fibroblasts constitute one of the largest noncardiomyocyte cell population (1). Fibroblasts, initially thought to be quiescent and nonreactive, transform into activated phenotype in response to inflammation and oxidant stress. However, recent studies show that resident fibroblasts continually influence cardiac homeostasis and are involved in extracellular matrix (ECM) maintenance (2, 3).

Fibroblasts under basal conditions play an important role in the maintenance of interstitial connective tissue and communication between cardiomyocytes. During ischemia, the cellular response mediated by fibroblasts and myofibroblasts can be classified into two types: replacement fibrosis and reactive fibrosis (4). Replacement fibrosis, that is, replacement of dead cardiomyocytes by formation of collagenous scar formation is a critical process to prevent rupture of the ventricular wall following cardiomyocyte death after an ischemic insult (2, 5, 6). Scar formation results in increased mechanical stress on the ventricular wall (7, 8). Along with the inflammation, increased mechanical stress induces overzealous long-term activation of fibroblasts and accumulation of ECM and connective tissue proteins in the infarct and the remote peri-infarct areas leading to reactive fibrosis. Triggering prolonged reactive fibrosis in the peri-infarct areas and in the remote relatively healthy myocardium alters ventricular compliance and increases ventricular stiffness, thus compromising cardiac diastolic function (9). Molecular alterations in the ischemic tissue, particularly in the peri-infarct area, determine the eventual infarct size and cardiac function.

The three classical components of the response to myocardial ischemia are inflammation, scar formation, and ECM remodeling, with overlap between individual components. After an acute ischemic event, the loss of tissue integrity stresses fibroblasts and induces their migration to the injured area, proliferation, and transformation into myofibroblasts (10). The activated fibroblasts express smooth muscle α-actin (αSMA) and vimentin, an intermediate filament protein, both widely used as myofibroblast makers (6, 7).

Correspondence: J. L. Mehta (mehtajl@uams.edu).
Submitted 13 May 2021 / Revised 17 August 2021 / Accepted 18 August 2021

Myofibroblasts, when activated serve as the primary collagen-producing cells mediating fibrosis. Myofibroblasts activation results from paracrine signals secreted by lymphocytes and macrophages, autocrine factors secreted by myofibroblasts, which interact with pattern recognition receptors (such as TLRs) on fibroblasts. Among the important regulators of fibrosis identified are the cytokines (such as IL-1β), chemokines, angiogenic factors, caspases (e.g., caspase-3), growth factors, and renin-angiotensin-aldosterone system (11).

Type 1 and 3 collagens along with fibronectin are the primary structural proteins in the cardiac extracellular matrix. They provide mechanical support by strengthening the myocardial wall and help in relaying the mechanical force of contraction (12). Fibroblasts and myofibroblasts synthesize and secrete collagens and fibronectin as precursor proteins that are converted to their mature fibrillar form by proteolytic cleavage by secreted proteinases. The mature fibronectin associates with extracellular proteins and self-assemble into fibrils providing a scaffold to which collagens and other ECM proteins bind (13–15). Profibrotic remodeling of cardiac ECM following an ischemic insult involves assembly of overexpressed fibronectin binding to intercellular cell surface adhesion molecules such as integrin. Inhibiting fibronectin expression inhibits fibrillar formation and attenuates adverse cardiac remodeling after ischemic insult and reduces scar formation (16).

There is an ongoing search for novel therapies to contain the infarct area. A promising novel area for intervention is the use of stem cell exosomes, which evidently reduce inflammation and limit cardiac systolic dysfunction (17–21). We have previously reported on the mechanism of cardioprotection mediated by MSC exosomes in ischemic mice hearts. There was a significant reduction in mediators of inflammation resulting in rescue of cardiac function and preservation of ventricular thickness with MSC exosome treatment (22).

The aim of our study was to understand the processes involved in scar formation in the ischemic hearts by studying the expression of ECM proteins in infarct and peri-infarct areas and how MSC exosomes might modulate these events.

MATERIALS AND METHODS

Cell Culture and Reagents

Cell culture media were obtained from Corning (Thermo Fisher Scientific, Waltham, MA), [penicillin-streptomycin, DMEM, phosphate-buffered saline (PBS)]. Fetal bovine serum (FBS) was obtained from Atlanta Biologicals Inc. (Flowery Branch, GA). Human cardiac fibroblast (306-05A HCF) cell line was obtained from Sigma-Aldrich (St. Louis, MO).

Culture of MSCs

The immortalized human bone marrow-derived MSC cell line (23–25) created from healthy donors was a gift from Dr. Robert J. Griffin at University of Arkansas for Medical Sciences. The MSCs were maintained in DMEM media (Thermo Fisher Scientific, Waltham, MA), supplemented with 10% FBS (Atlanta Biologicals Inc., Flowery Branch, GA) and penicillin-streptomycin (100 U/mL obtained from Thermo Fisher Scientific, Waltham, MA) in a 5% CO_2 incubator at 37°C. In brief (26), cells were cultured overnight and then washed with PBS and fresh serum-free DMEM medium was added. The cells were cultured for a further 16–18 h at 37°C in a 5% CO_2 incubator. Culture media from these cells was collected for exosome isolation.

Exosome Isolation

Exosomes were isolated from culture media of MSC cultures incubated in serum-free DMEM media for 16–18 h by sequential centrifugation as previously described (27). In brief, media pooled from MSC cultures was subjected to a series of centrifugation steps, first at 3,000 *g* for 10 min followed by centrifugation for 30 min at 10,000 *g*. The pellets were discarded and followed by ultracentrifugation at 100,000 *g* for 3 h to pull down exosomes. The resulting exosome pellet was resuspended in PBS for washing and ultracentrifuged for 2 h at 100,000 *g*. The final pellet thus obtained was resuspended in PBS and used in experiments.

Exosome Characterization

MSC exosomes were imaged using the JEOL JSM7000F scanning electron microscope as previously described (28). Western blots for CD9 (No. EXOAB-CD9A-1) and CD63 (No. EXOAB-CD63A-1) (markers for exosomal vesicles) were used to further characterize the isolated vesicles. Finally, nanoparticle tracking analysis (NTA) using the ZetaView PMX 110 (Particle Metrix, Meerbusch, Germany) was used to characterize and study size distribution of isolated vesicles, as previously reported (26).

Acute and Chronic Ischemia Mouse Models

Adult male C57BL/6 mice were obtained from the Jackson Laboratory (Bar Harbor, ME). The animal study protocol (No. 1466223) was approved by the local institutional animal use care committee and conformed to the *Guide for the Care and Use of Laboratory Animals* published by the National Academies Press (Washington, DC). The 8- to 10-wk-old mice used in the experiments were euthanatized by CO_2 inhalation at the end of 7 days after LCA ligation. For purposes of this study, we characterize 1-h ischemia as acute ischemia and LCA ligation for 7 days as chronic ischemia.

Acute myocardial ischemia (brief) was induced by total LCA occlusion in the anesthetized mice as described previously (29, 30). In brief, following ketamine hydrochloride (60 mg·kg^{-1}) and xylazine hydrochloride (8 mg·kg^{-1}) administered intraperitoneally, the anesthetized animals were endotracheally intubated and mechanically ventilated (1.2 mL·min^{-1} tidal volume and 110/min respiration rate). An 8-0 silk suture was passed around the LCA at a point two-third of the way between its origins near the pulmonary conus. After 1 h of ischemia, the ligature around the LCA was released to allow for reperfusion, and the animals were euthanized 3 h later. Another group of animals underwent the same procedure but without LCA occlusion (sham ischemia). A third group of mice was pretreated with a single dose of MSC exosomes (0.5 mg/kg body wt, administered intravenously through the lateral tail vein) 30 min before left coronary artery (LCA) ligation. The quantity of MSC exosomes

administered to the animals was based on previous studies (31, 32).

Chronic myocardial ischemia was induced by permanent LCA ligation for 1 wk. A parallel group of animals underwent the same procedure, but without LCA ligation (sham ischemia). A third group of mice was pretreated with a single dose of MSC exosomes as described in *Acute and Chronic Ischemia Mouse Models*.

Masson's Trichrome Staining

Mice hearts were collected after euthanasia and fixed in 10% formalin solution and embedded in paraffin. The hearts were subsequently sliced into 5-μm thick slices from base to apex. The sections were deparaffinized in xylene and rehydrated through gradient ethanol (100% to 70%) and stained with Masson's trichrome per standard protocols. The collagen fibers were stained blue, the nuclei were stained black, and myocardium was stained red. Bright-field images were acquired using the Olympus Bx40 light and fluorescent microscope. Infarct areas were identified, and regions of interest within the infarct areas were randomly selected from multiple sections of at least five mice in each group and the extent of fibrosis was quantified by processing the acquired images with Image J software.

Assessment of Inflammatory Signals by Immunofluorescence Staining

Formalin-fixed hearts were sectioned into 3–5 regions, and then 5-μm thick slides from different regions of the heart (3 mice in each group) were deparaffinized. For immunofluorescence staining, deparaffinized heart sections were permeabilized with 1% Triton X-100. The sections were blocked with 5% goat serum-1% BSA in PBS for 30 min at room temperature and then incubated with specific antibodies. Images were acquired using the Olympus microscope and processed using the Image J software to merge and adjust the brightness and contrast present the staining. Brightness and contrast of the merged images was further adjusted using MS PowerPoint before being saved as TIFF images for final figures. Infarct and peri-infarct areas were identified using subsequent hematoxylin-eosin-stained slices of mice hearts as reference areas to image fluorescent staining. Fluorescence intensities of inflammatory markers and pathway mediators were quantified using ImageJ software in multiple areas from six mice in each group.

Mass Spectrometry

The freshly isolated heart tissues were homogenized in a homogenizer and total protein was extracted using a lysis buffer. The lysates were then subjected to mass spectrometric analysis. For mass spectrometry identification and analysis, refer to the previously described method (26). Scaffold 4 software was used for peptide and protein identifications. Acceptable limits for protein identifications were at least two identified peptides with less than 1.0% false discovery. Scaffold Q+ (version Scaffold 4.8.9, Proteome Software, Inc., Portland, OR) was used for analysis with protein threshold cutoffs of 95%, minimum of 2 peptides, and a 50% peptide threshold values. The file can be accessed using the following link: https://doi.org/10.6084/m9.figshare.14550978. The list of proteins identified was uploaded into the ingenuity pathway analysis (IPA) software and comparative analysis of proteins from different hearts was performed.

SDS-PAGE and Western Blotting

Infarct and peri-infarct areas were carefully dissected from freshly isolated hearts from euthanized mice, homogenized in a homogenizer, and total protein was extracted using a lysis buffer. Western blotting was performed using standard procedures (26). Membranes were incubated with primary antibodies against IL-1β (No. ab9722-rabbit polyclonal antibody at 1:1,000 dilution), fibronectin (No. ab2413-rabbit polyclonal antibody at 1:1,000 dilution) (all from Abcam, Cambridge, MA), NLRP3 (No. 15101-rabbit monoclonal antibody at 1:1,000 dilution), NF-κB (No. 8242-rabbit monoclonal antibody at 1:1,000 dilution), ASC (No. 67824-rabbit monoclonal antibody at 1:1,000 dilution), superoxide dismutase 1 (SOD1; No. 37385-rabbit monoclonal antibody at 1:1,000 dilution), Collagen-1 (No. 72026-rabbit monoclonal antibody at 1:1,000 dilution), Collagen-3 (No. 30565-rabbit polyclonal antibody at 1:1,000 dilution), Vimentin (No. 5741-rabbit monoclonal antibody at 1:1,000 dilution), α-SMA (No. 19245-rabbit monoclonal antibody at 1:1,000 dilution), matrix metalloproteinase 2 (MMP2; No. 40994-rabbit monoclonal antibody at 1:1,000 dilution), MMP9 (No. 13667-rabbit monoclonal antibody at 1:1,000 dilution), tissue inhibitor of metalloproteinase 2 (TIMP2; No. 5738-rabbit monoclonal antibody at 1:1,000 dilution) (all from Cell Signaling Technology, MA), CD63 (No. EXOAB-CD63A-1, rabbit polyclonal antibody at 1:1,000 dilution) (SBI Biosciences, Mountain View, CA), and against β-actin (No. ab8226) and GAPDH (No. ab9484) (both mouse monoclonal antibody at 1:5,000 dilution) (Abcam, Cambridge, MA) for 1 h at room temperature. Blots were washed three times with TBS-t and then incubated with anti-mouse (No. 7076) or anti- rabbit (No. 7074) antibody conjugated with horseradish peroxide (at 1:10,000 dilution) (Cell Signaling Technology) at room temperature for 1 h. Blots were rinsed three times with TBS-t and developed with a chemiluminescence developing reagent51, SuperSignal West Femto Maximum sensitivity substrate (Thermo Fisher Scientific, Rockford, IL). The protein bands were scanned and quantified using Image J software. The full-length images of the blots are given in Supplemental Fig. S1 (all Supplemental material is available at https://doi.org/10.6084/m9.figshare.14550978).

Cell Viability and Death Assay

Fibroblasts were cultured to a near confluence (~90%) in 96-well plates overnight in DMEM medium. One set of cells was left untreated, whereas one set of cells was treated with lipopolysaccharide (LPS) for 1 h. Another set of cells was then treated with MSC exosomes alone, whereas MSC exosomes were added to one set of LPS-treated cells. Amount of LDH release was quantified using the LDH cytotoxicity assay kit (Cayman Chemical, Ann Arbor, MI) following the manufacturer's protocol. Cell viability assay was carried out on a similar set of treated and untreated fibroblasts using MTT reagent (Invitrogen, Eugene, OR) following the manufacturer's protocol.

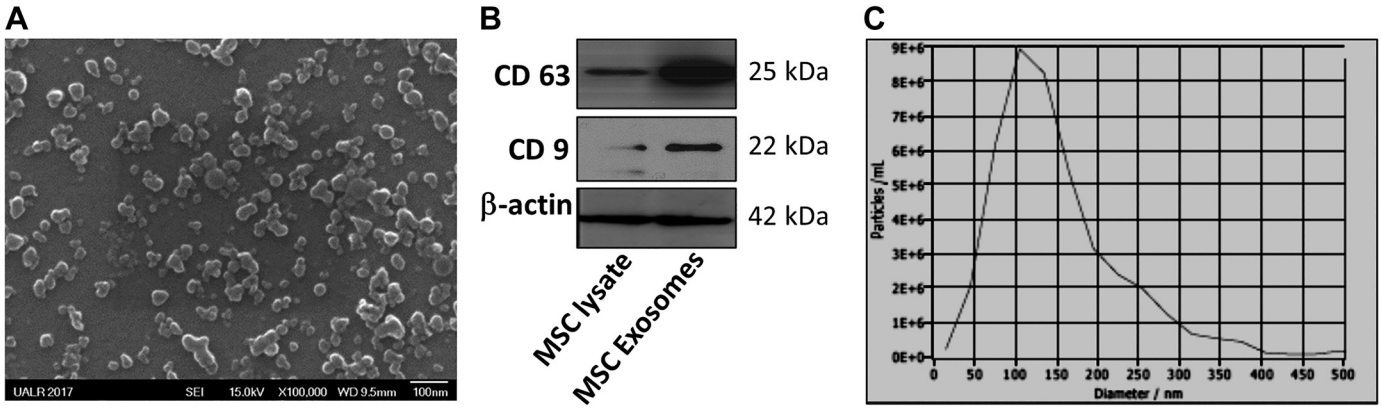

Figure 1. Characterization of MSC exosomes. SEM of MSC exosomes fixed on fibronectin-coated coverslip (approx. ~80 nm), scale bar = 100 nm (*A*). CD63 and CD9 (exosomal markers) are detected in significant quantity in the exosome prep, whereas barely detected in MSC cell lysates (*B*). NTA (ZetaView measurements of MSC exosomes) analysis to measure hydrodynamic diameters and size distribution (in mm) of exosome vesicles isolated from MSC cultures (*C*). MSC, mesenchymal stem cell; NTA, nanoparticle tracking analysis; SEM, scanning electron microscopy.

Cell Migration Assay

Fibroblasts were cultured in a QCM Chemotaxis 96-Well Cell Migration Assay kit with a pore size of 8 μm (Millipore). In brief, 150 μL of DMEM media was added to the wells of the feeder tray in triplicate. Five thousand fibroblast cells were added to the insert. Cells were then washed and fresh serum-free DMEM medium was added. Cells were treated with LPS for 1 h and then with MSC exosomes, either alone or in presence of LPS, and allowed to migrate for 12 h. Migrated cells from the bottom of the inserts were then fixed with 4% paraformaldehyde solution in PBS and nuclei were stained with Hoechst. The inserts were imaged under a fluorescent microscope and the number of nuclei were counted in three fields from each of the replicates and tabulated and presented as number of cells in each field counted.

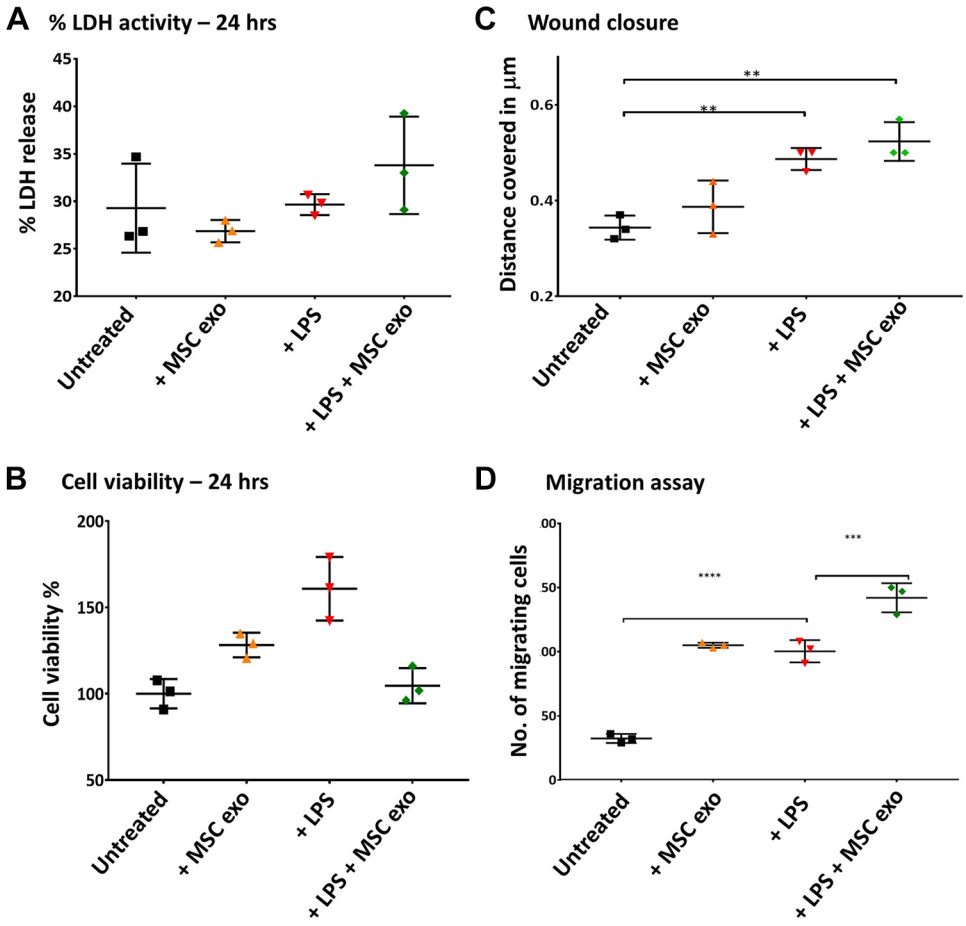

Figure 2. Effect of MSC exosomes on fibroblast activity. LPS stimulation of fibroblasts had no detrimental effect on either cell death (*A*) or survival (*B*). However, both LPS and LPS + MSC exosomes increased fibroblast migration (*C*). MSC exosomes also increased invasiveness of the fibroblasts in presence of LPS (*D*). Data in means ± SD, $^{**}P < 0.01$,$^{***}P < 0.001$, $^{****}P < 0.0001$ based on 3 independent experiments. LPS, lipopolysaccharide; MSC, mesenchymal stem cell.

Migration-Scratch Assay

Fibroblasts were cultured to a near confluence (~90%) in 6-well plates overnight in DMEM medium. With the use of a pipet tip, scratches were made in the cell layer; cells were then washed with PBS (3 times) and fresh serum-free DMEM medium was added. One set of cells was left untreated, whereas two sets of cells were treated with LPS for 1 h. Another set of cells was then treated with MSC exosomes alone, whereas MSC exosomes were added to one set of LPS-treated cells. Phase contrast images were recorded on a Cytation 5 imaging reader (BioTek) at 0, 3, and 7 h. Scratch widths from six areas of each scratch were measured using Image J software. Values at each timepoint were first subtracted from 0 h and then divided by the same and reported as ratio of area filled; data presented are for the 7-h timepoint.

Statistical Analysis

We used GraphPad Prism's one-way ANOVA followed by Tukey's multiple comparison test to calculate statistical significance for fibroblast cell results, quantification of interstitial fibrosis, and mice heart protein levels expressed as means ± SD. Value of $P < 0.05$ was considered significant. The experiments conducted and results analyzed in this study were nonblinded.

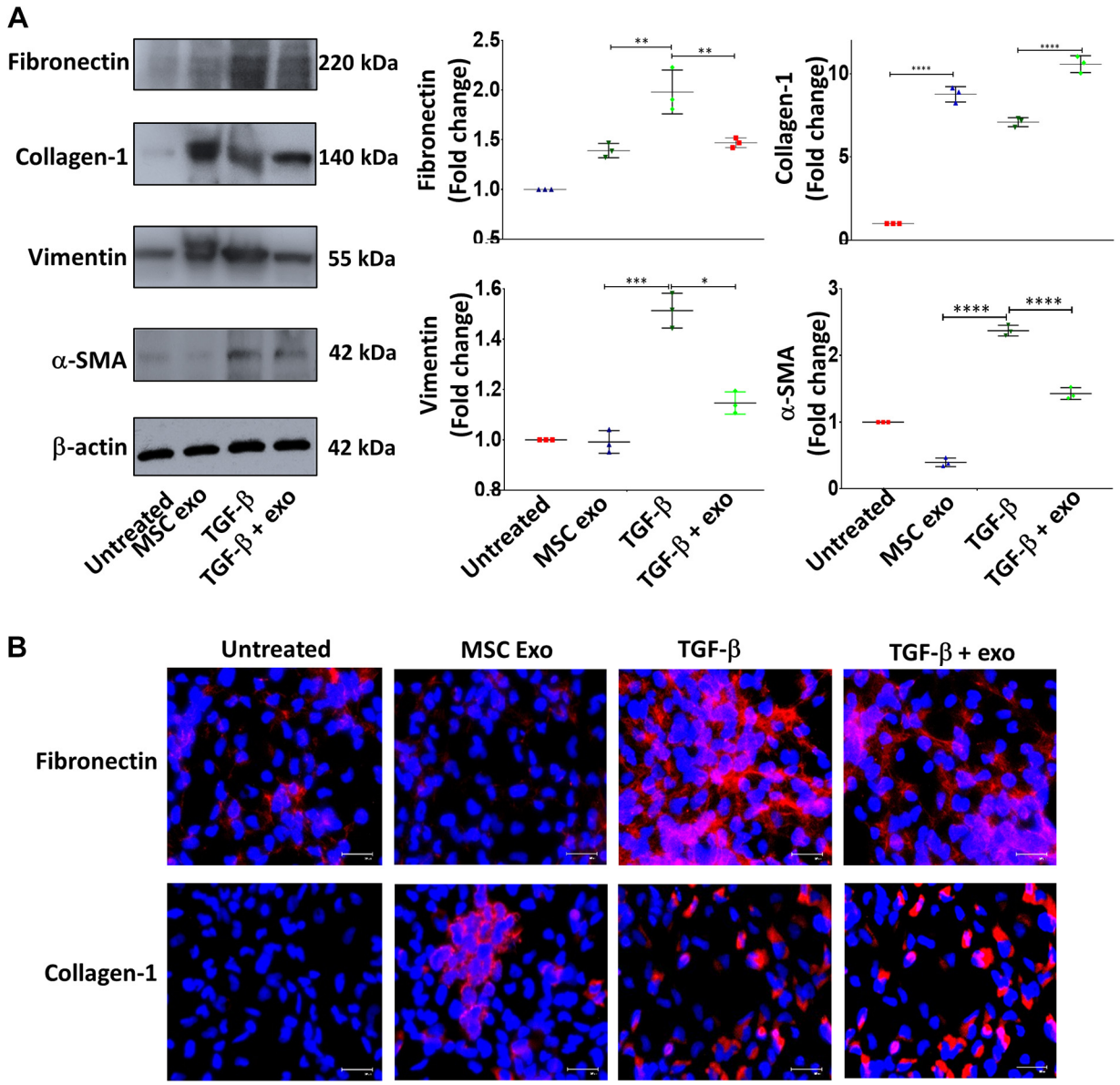

Figure 3. MSC exosome-mediated suppression of fibrosis in fibroblasts. Fibroblast cultures were exposed to TGF-β (10 ng/mL) for 1 h and then treated with MSC exosomes. TGF-β-induced fibronectin, collagen-1, vimentin, and α-SMA expression at 24 h of exposure. *A*: MSC exosome treatment decreased fibronectin, vimentin, and α-SMA levels in fibroblasts stimulated with TGF-β over a period of 24 h. Immunofluorescence images also showed a decrease in fibronectin and collagen-1 expression in fibroblasts treated with MSC exosomes (*B*). Data in means ± SD as fold change over untreated cells, $n = 3$ replicates. *$P < 0.05$, **$P < 0.01$, ***$P < 0.001$, ****$P < 0.0001$ based on 3 independent experiments. Scale bar = 50 μm. Full-length blots are presented in Supplemental Fig. S1C. MSC, mesenchymal stem cell; α-SMA, smooth muscle actin-α.

RESULTS

Characterization of Exosomes

We have previously described characterization of MSC exosomes using scanning electron microscopy (SEM), nanoparticle tracking analysis, and Western blotting (26). With the use of an 80-keV electron beam, micropictographs obtained by scanning electron microscopy showed presence of uniform size and diameter vesicles (Fig. 1). Mass spectrometry analysis revealed the absence of several organelle markers such as endoplasmic reticulum marker calnexin, golgi marker GM130, mitochondrial marker proteins such as cytochrome c oxidase, ABCD3, ATP5A1, etc. MS analysis revealed the presence of several exosomal markers such as CD63, CD9, and CD81 [for MSC exosome proteomics refer supplementary data set from Kore et al. (26)]. These results along with electron micropictographs indicate that the pellets isolated from conditioned media of MSC cultures by sequential centrifugation constitute a distinct set of secretory vesicles.

In Vitro Activation of Cultured Fibroblasts

Since inflammation is a major component of ischemic injury to the heart, we investigated the influence of a potent proinflammatory mimic LPS on migration capability of cultured fibroblasts in a scratch/wound-healing assay. Fibroblasts were plated with or without MSC exosomes in the presence or absence of LPS. Significant stimulation of wound healing in scratch assay was seen when fibroblasts were stimulated with LPS (Fig. 2*C*). A similar significant stimulation of fibroblast migration was observed in the presence of LPS (Fig. 2*D*).

Treating the fibroblasts with MSC exosomes in the presence of LPS had no effect on cell death, whereas cell survival was similar to untreated fibroblasts (Fig. 2, *A* and *B*). Compared with the LPS-treated cells, MSC exosome treatment had no effect on scratch/wound-healing function of fibroblasts (Fig. 2*C*). However, the exosomes significantly induced fibroblast migration across a porous permeable membrane, suggesting MSC exosomes stimulate invasive function in fibroblasts. There was a further increase in migration of LPS-stimulated fibroblasts in the presence of MSC exosomes (Fig. 2*D*). These results suggest that MSC exosomes stimulate migration capability of the fibroblasts. We monitored LDH activity as a marker of cell death at 24 h in the presence of LPS (Fig. 2*A*). Interestingly, cell viability measured by MTT assay increased under the stress of LPS (Fig. 2*B*), perhaps a response to stress. MSC exosomes in the presence of LPS had normalized the LDH levels.

Cultured fibroblasts treated with 10 ng/mL of tumor necrosis factor-β (TGF-β), which is another potent cytokine released during ischemia (Fig. 3, *A* and *B*), revealed upregulation of fibrosis markers fibronectin and collagen-1 and myofibroblast markers smooth muscle actin-α (α-SMA) and vimentin. MSC exosome treatment alone had no

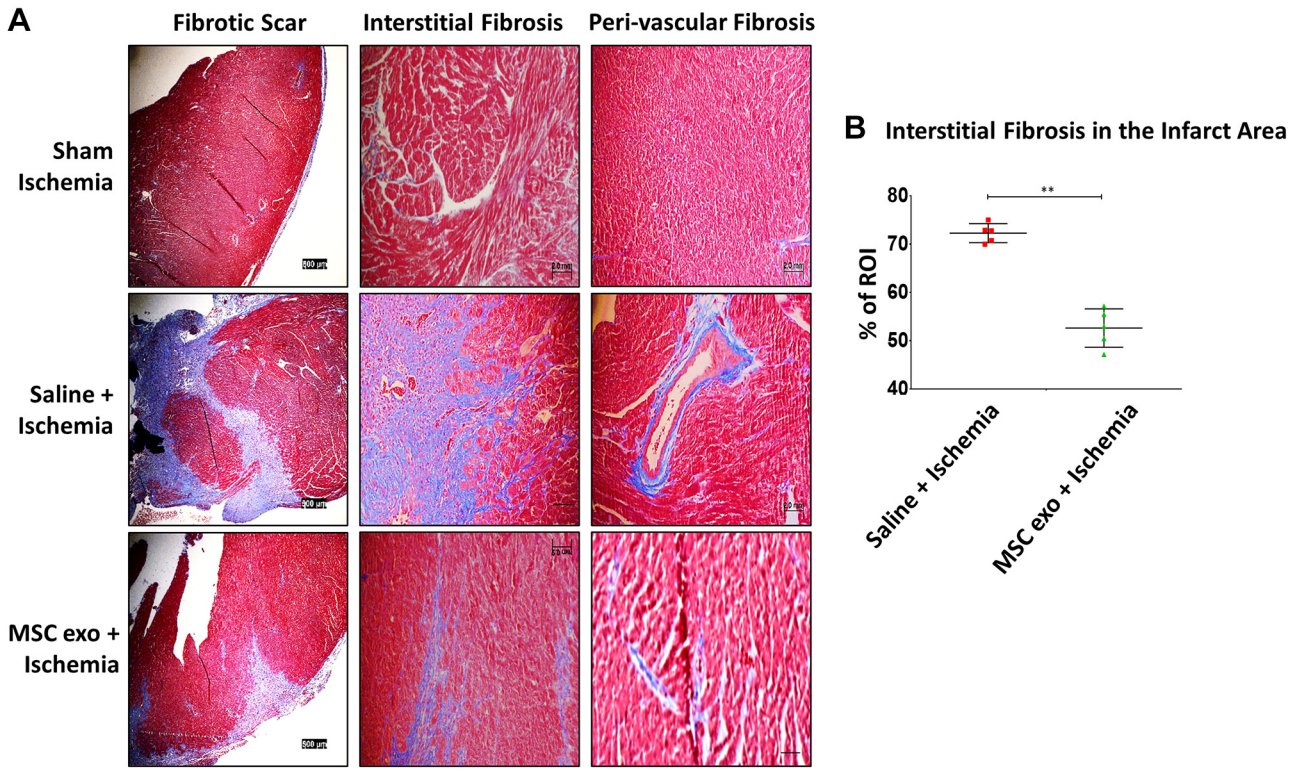

Figure 4. Interstitial fibrosis in chronic ischemia. Masson's trichrome staining shows significant fibrotic scar formation in the ischemic hearts (1-wk post-LCA ligation), especially in the infarct areas (*A* and *B*). There is prominent perivascular fibrosis observed in the saline-treated hearts (*A*). With MSC exosome treatment, there is a significant decrease in interstitial fibrosis in ischemic hearts along with a decrease in perivascular fibrosis. Data in means ± SD, from multiple regions of interest (ROI) from $n = 5$ mice hearts. Scale bars: fibrotic scar = 500 μm; interstitial fibrosis and perivascular fibrosis = 2 mm. Multiple comparisons were analyzed by one-way ANOVA, followed by Tukey's post hoc comparisons test (**$P < 0.01$). MSC, mesenchymal stem cell.

effect on fibronectin or vimentin expression in fibroblasts, whereas it surprisingly upregulated collagen-1 and suppressed α-SMA expressions (Fig. 3, *A* and *B*). MSC exosomes significantly suppressed fibronectin, vimentin, and α-SMA in the presence of TGF-β. Interestingly, treating fibroblasts with MSC exosomes in presence of TGF-β induced a small but significant increase in collagen-1 expression.

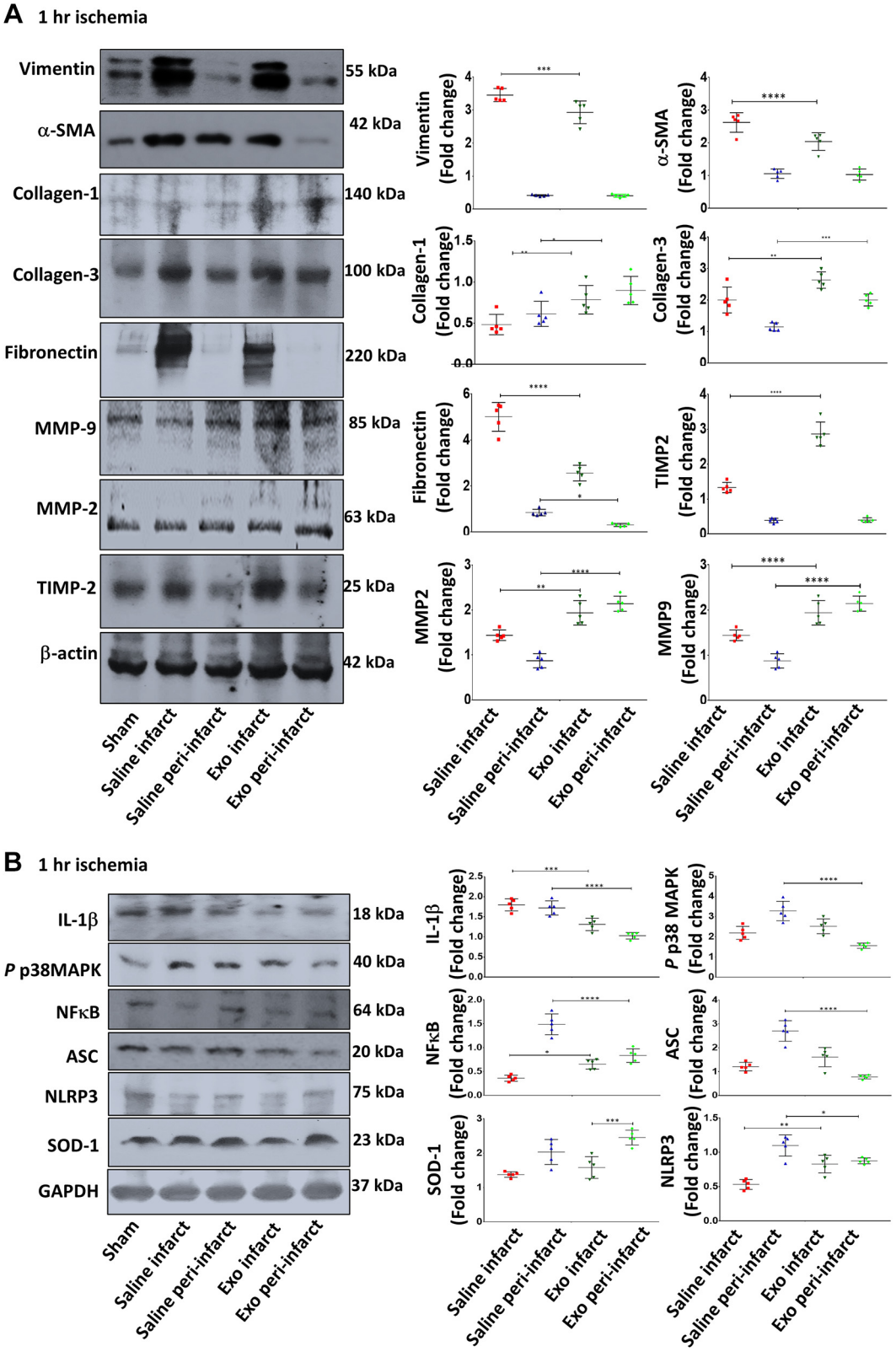

Effect of MSC Exosomes on ECM Protein Secretion during Acute Ischemia

We then induced ischemia in mice hearts with LCA ligation. One week later, the ischemic hearts were collected. Masson's trichrome staining of chronic ischemia hearts showed profound fibrotic scar tissue and ECM proteins in the infarct areas. After MSC exosome treatment, both interstitial fibrosis (Fig. 4, *A* and *B*) and perivascular fibrosis in ischemic hearts were significantly decreased (Fig. 4).

We looked at the molecular events occurring immediately and 1 wk after the induction of ischemia. The expression of vimentin and α-SMA, markers for myofibroblasts, was markedly increased in the infarct areas shortly after the ischemic insult. There appeared to be a very small quantity of vimentin detected in the peri-infarct areas. Next, we investigated the expression of markers of fibrotic scar tissue. There was a significant increase in the expression of fibronectin and collagen-1 and -3 soon after a brief period of ischemic insult. We also observed an increase in the secretion of TIMP2, MMP2, and MMP9, especially in the infarct areas, which are involved in turnover of ECM proteins (Fig. 5*A*).

MSC exosome treatment significantly reduced fibronectin expression in both infarct and peri-infarct areas. The expression of myofibroblast markers, vimentin and α-SMA, was also significantly suppressed in the infarct and peri-infarct areas of MSC exosome-treated ischemic mice hearts. However, surprisingly, levels of collagen-1 and -3, MMP2, and MMP9 were increased with MSC exosome treatment in the infarct and peri-infarct areas. Although TIMP2 levels were increased in the infarct areas, their levels in the peri-infarct areas were not affected (Fig. 5*A*).

Effect of Acute Ischemia on Inflammatory Mediators and Rescue by MSC Exosomes

We examined expression of a well-known potent inflammatory modulator IL-1β in the cardiac tissues following a brief period of ischemia. We observed a marked upregulation of IL-1β in both the infarct and peri-infarct areas (Fig. 5*B*) within a few hours of the ischemic insult. Activation of inflammatory signals was accompanied by the activation of intracellular inflammatory proteins p38-MAPK, NF-κB, ASC, and NLRP3 inflammasome (Fig. 5*B*). SOD1 expression increased after brief period of ischemia, and its levels were higher in the peri-infarct areas than in infarct areas.

Importantly, MSC exosome treatment significantly decreased the levels of inflammatory modulators IL-1β along with suppression of phospho-p38-MAPK, NF-κB, and NLRP3 inflammasome. The levels of SOD1 increased further with MSC exosome treatment (Fig. 5*B*). It is interesting to note that SOD1 levels in the peri-infarct areas were significantly higher than in the infarct areas of MSC exosome-treated mice hearts.

Effect of MSC Exosomes on ECM Protein Secretion and Inflammatory Mediators during Chronic Ischemia

Next, we studied cardiac ECM remodeling at 1 wk of ischemia. There was an increased deposition of collagen-1 and -3 along with increased staining for the myofibroblast markers vimentin and α-SMA (Fig. 6*A*). Levels of MMP2 and TIMP2 area were also increased (Fig. 6*A*), suggesting that the trends observed during acute ischemia continue over a period of time. MSC exosome treatment, as expected, showed a decrease in vimentin and α-SMA staining in the chronic ischemic hearts. However, levels of both collagen-1 and -3 and MMP2 and TIMP2 were increased in both infarct and peri-infarct areas.

The trend of increased expression of inflammatory markers such as IL-1β, NF-κB, and NLRP3 was evident in mice hearts subjected to chronic ischemia in both infarct and peri-infarct areas with increased staining observed in the peri-infarct areas. There was increased staining of NF-κB within the nucleus in both infarct and peri-infarct areas of saline-treated mice heart areas indicating its activation and localization to the nucleus (Fig. 6*B*), although the staining was more prominent in the peri-infarct regions. The suppression of these inflammatory mediators with MSC exosome administration was evident in chronic ischemia hearts in both infarct and peri-infarct areas (Fig. 6*B*).

Proteomic Analysis of Ischemic Hearts

Mice hearts with LCA ligation for 1 wk were carefully homogenized, lysed, and protein extracted and subjected to mass spectrometric (MS) analysis.

We studied the pathways governing fibrosis using Ingenuity pathway analysis (IPA) (33) of proteome of these hearts. Our investigation revealed the proteins involved in the toxicological functions (Fig. 7*A*) and diseases and biological functions (Fig. 7*B*) and showed differential expression of upstream regulators of cellular signaling (Fig. 7*C*). Saline-treated ischemic hearts showed an increase in proteins regulating fibrogenesis and fibrosis of heart. Treatment of mice with MSC exosomes was found to suppress the pathways governing fibrosis of heart and decrease fibrogenesis and ventricular dysfunction pathways. Proteins regulating angiogenesis were stimulated with MSC exosome treatment (Fig. 7*B*). We also observed differential regulation of many transcription factors. Most interestingly, there was a suppression of the nuclear receptor subfamily 4 group A member 1 (NR4A1), whereas nuclear receptor subfamily 1 group I

Figure 5. Fibrosis and inflammatory mediators during acute ischemia. Vimentin and α-SMA levels are significantly elevated during acute ischemia (*A*) indicative of increased fibroblast transformation to myofibroblasts. Collagen-1 and -3 levels along with fibronectin and MMP2, MMP9, and TIMP2 are also elevated during acute ischemia. MSC exosome treatment significantly reduces fibrotic response in ischemia hearts (*A*). Similarly, after 1 h of ischemia, IL-1β, phosphorylated-p38MAPK, NF-κB, ASC, NLRP3, and SOD1 levels are increased in both infarct and peri-infarct areas (*B*). MSC exosome treatment reduces levels of these inflammatory mediators and inflammasome proteins in the heart tissues. MSC exosomes also increase levels of SOD1 and these protective effects persist during chronic ischemia (*B*). Data in means ± SD, presented as fold change over sham heart lysates, $n = 5$. Multiple comparisons were analyzed by one-way ANOVA, followed by Tukey's post hoc comparisons test (*$P < 0.05$, **$P < 0.01$, ***$P < 0.001$, ****$P < 0.0001$). Full-length blots are presented in Supplemental Fig. S1, *A* and *B*. MMP2, matrix metalloproteinase 2; MMP9, matrix metalloproteinase 2; MSC, mesenchymal stem cell; SOD1, superoxide dismutase 1; TIMP2, tissue inhibitor of metalloproteinase 2; α-SMA, smooth muscle actin-α.

member 3 (NR1I3) was elevated with MSC exosome treatment (Fig. 7*C*).

The IPA analysis revealed IL-1β as the major cytokine mediator regulating fibrosis in ischemic hearts leading to stimulation of vimentin, DDX5, and fibronectin, which promote fibrosis (red circles Fig. 7*D*) while also stimulating SOD (light blue circle Fig. 7*D*), which suppresses oxidative stress-driven profibrotic pathways. The increase in SOD may be a

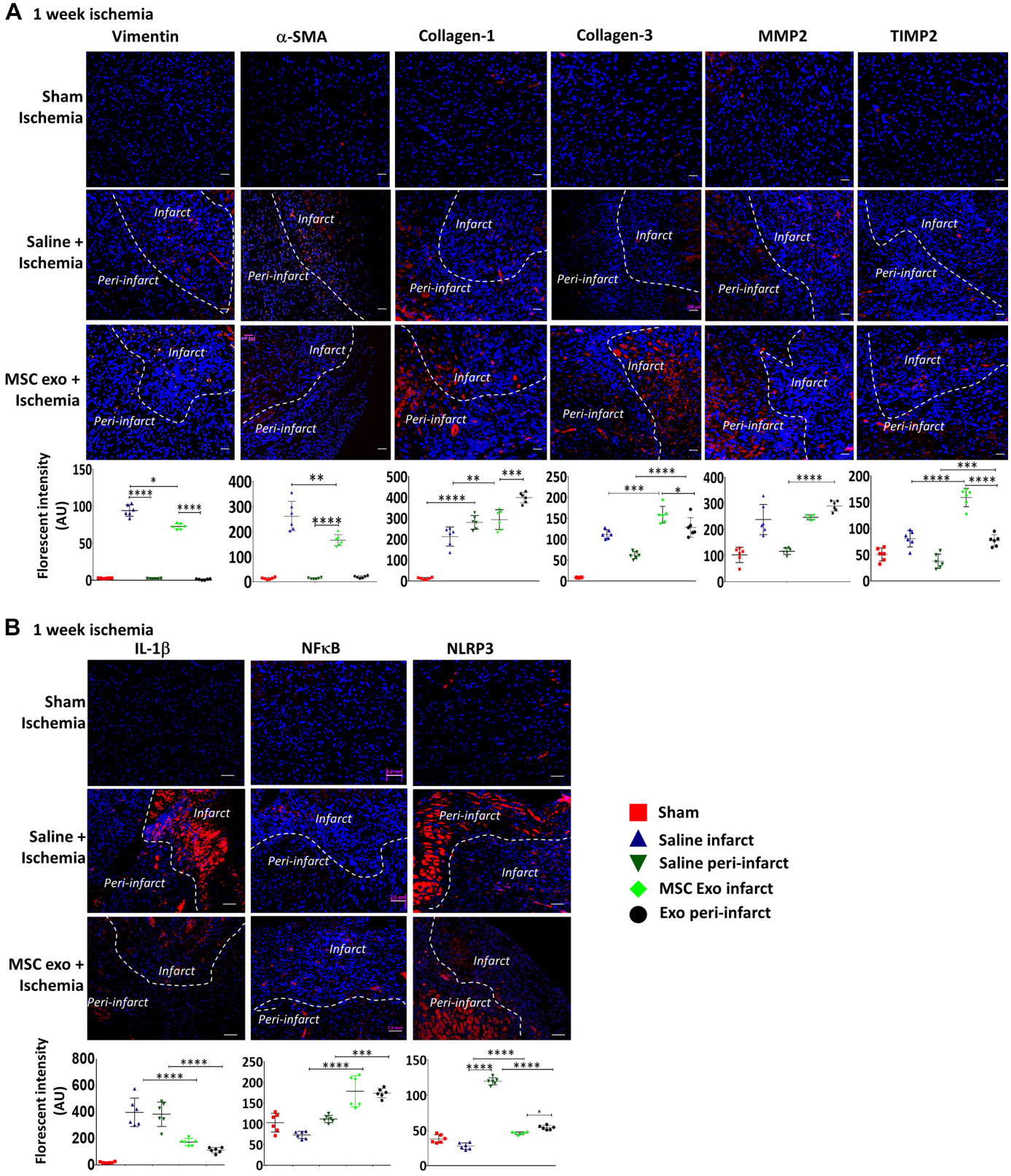

compensatory response to increase in profibrotic and proinflammatory pathways, as seen earlier (34, 35). We suspect that the suppression of NR4A1 would lead to increase in collagen-1 levels (36, 37), which corroborates the data shown in Fig. 7*E*.

A further detailed analysis of the saline-treated ischemic hearts and MSC exosome-treated ischemic hearts revealed differences in the proteins involved in fibrogenesis (Fig. 8, *A* and *B*) and fibrosis of heart pathways (Fig. 8, *C* and *D*). Comparative analysis of the process of fibrogenesis in saline-treated mice hearts subjected to LCA ligation revealed differentially expressed proteins such as MyoZ2, THBS1, TTR, SERPINF2, DMD, PKP2, SORBS1, DCTN1, MAPK1, Cyb5r3, DPYSL2, PFN1, HSPB1, and GDA (Fig. 8*A*). In contrast, the proteome of MSC exosome-treated heart tissues revealed fewer proteins involved in fibrogenesis with DLG1, Cdc42, CLASP1, PTPN11, MAPRE1, SNX9, and TNNT2 being differentially expressed (Fig. 8*B*). A similar analysis in saline-treated mice hearts subjected to LCA ligation revealed differentially expressed proteins such as PLG, SLC4A1, XIRP1, DMD, and PPP3CA, which play a role in the fibrosis of heart (Fig. 8*C*). Analysis of the proteome of MSC exosome-treated heart tissues identified unique set of proteins (SLC8A1, IGHM, GNAS, TNNT2, and COQ9) involved in modulation of fibrosis in the ischemic heart (Fig. 8*D*).

DISCUSSION

Previous work from several laboratories, including ours, has shown that ischemic insult to the heart triggers release of proinflammatory mediators, IL-1β, IL-6, and TNF-α (30, 38–42). Inflammation drives generation of reactive oxygen species (ROS) in the cytoplasm and mitochondria (43, 44). Activation of proinflammatory p38MAPK pathways, translocation of NF-κB, and transcription of IL-1β, NLRP3 inflammasome, and caspases further drive the vicious cycle leading to myocardial damage. The present study confirms these processes (Figs. 5 and 6). We also found that acute ischemia increased levels of the antioxidant SOD1, which is probably a compensatory response to counter ROS production.

Our study, for the first time, shows that the levels of mediators of inflammation—p38MAPK, IL-1β, and NLRP3 inflammasome—are elevated to a greater extent in the ischemic heart, more in the peri-infarct areas than in the infarct areas (Figs. 5 and 6). This surge in inflammatory mediators in the peri-infarct areas is possibly in response to inflammatory signals and cellular debris flooding from the infarct area. Not surprisingly, SOD1 expression increases to combat the ischemic stress. Furthermore, the inflammatory process with enhanced expression of IL-1β, NF-κB, and NLRP3 inflammasome continues during the chronic phase (Figs. 5 and 6).

To understand whether fibroblasts are directly influenced by MSC exosomes, we stimulated fibroblasts with the potent inflammatory stimulant LPS. Our in vitro investigation designed to study the fibrosis-related events revealed that LPS did not induce cell death in fibroblasts but slightly increased their cell viability, which probably reflects an inherent response of fibroblasts to inflammatory stimuli. LPS did activate fibroblast migration and although MSC exosome treatment further increased the migration of fibroblasts (Fig. 2, *C* and *D*), their transformation into activated myofibroblasts was suppressed (Figs. 5 and 6). When we treated fibroblasts with TGF-β (a potent cytokine that mediates fibrosis in damaged cardiac tissues), it resulted in an increase in expression of vimentin, α-SMA, and secretion of collagen-1 and fibronectin (Fig. 3). MSC exosome treatment suppressed levels of vimentin, α-SMA, and secreted fibronectin in cultured fibroblasts while stimulating the expression of collagen-1, suggesting that MSC exosomes act directly on cardiac fibroblasts to suppress fibrotic events in ischemic hearts.

It is well known that during acute ischemia, tissue response to inflammation and oxidative stress increases the production of ECM proteins involved in profibrotic remodeling. Fibroblasts transform into active myofibroblasts in the inflammatory microenvironment. Myofibroblasts express vimentin and secrete fibronectin (Figs. 5 and 6). Fibronectin, the anchor protein that binds to the cell surface and cross links with collagens, is secreted in large amounts by fibroblasts in response to ischemia (Fig. 3). Collagen-1 and -3 levels are also elevated which result in turnover of cardiac ECM to progressive fibrosis (Fig. 5). Although the ultimate fate of myofibroblasts is unknown, they flourish in the ischemic environment driving fibrosis. Fibrosis progresses after the initial ischemic insult and continues to progress.

Collagen-1 and -3 levels are elevated which result in turnover of cardiac ECM to progressive fibrosis (Figs. 5 and 6). Although the ultimate fate of myofibroblasts is unknown, they flourish in the ischemic environment driving fibrosis. Fibrosis progresses after the initial ischemic insult and continues to progress over a period.

Among the proteases involved in ECM turnover are MMP2, MMP9, and TIMP2. An increase in collagen secretion stimulates increased MMP2 and MMP9 secretion and increased fibrosis. A consequence of rapid MMP2 secretion in response to ischemia is the secretion of TIMP2 that processes MMP2. We also observed a rapid increase in TIMP2 secretion following the acute ischemic insult in mice hearts (Figs. 5 and 6). Our studies provide support for the concept of signals for fibrosis appearing soon after ischemia, first postulated by Hu et al. (41) in our laboratory.

Ischemic insult kills cells in the infarct areas (Fig. 4). Fibroblasts move into the area and secrete profibrotic ECM proteins to maintain the structural integrity of the damaged heart tissue leading to scar formation. In the peri-infarct areas, the levels of ECM proteins, although increased, are significantly lower than those in the infarct areas. We hypothesize that the increased levels of collagen-1 and -3 are a

Figure 6. Fibrosis and inflammatory mediators during chronic ischemia. At 7 days after left coronary artery (LCA) ligation (lig) in chronic ischemia model, Vimentin and α-SMA levels are significantly elevated (*A*) indicative of increased fibroblast transformation to myofibroblasts. Collagen-1 and -3 levels along with MMP2 and TIMP2 are also elevated. These protective effects of MSC exosome treatment persist during chronic ischemia (*A*). Inflammatory mediators such as IL-1β, NF-κB, and NLRP3 levels are increased in both infarct and peri-infarct areas (*B*). MSC exosome treatment reduces levels of these inflammatory mediators and inflammasome proteins in the heart tissues (*B*). Data in means ± SD, as florescent intensities (arbitrary units), $n = 5$. Scale bars = 2 mm. Multiple comparisons were analyzed by one-way ANOVA, followed by Tukey's post hoc comparisons test (*$P < 0.05$, **$P < 0.01$, ***$P < 0.001$, ****$P < 0.0001$). MMP2, matrix metalloproteinase 2; MSC, mesenchymal stem cell; TIMP2, tissue inhibitor of metalloproteinase 2; α-SMA, smooth muscle actin-α.

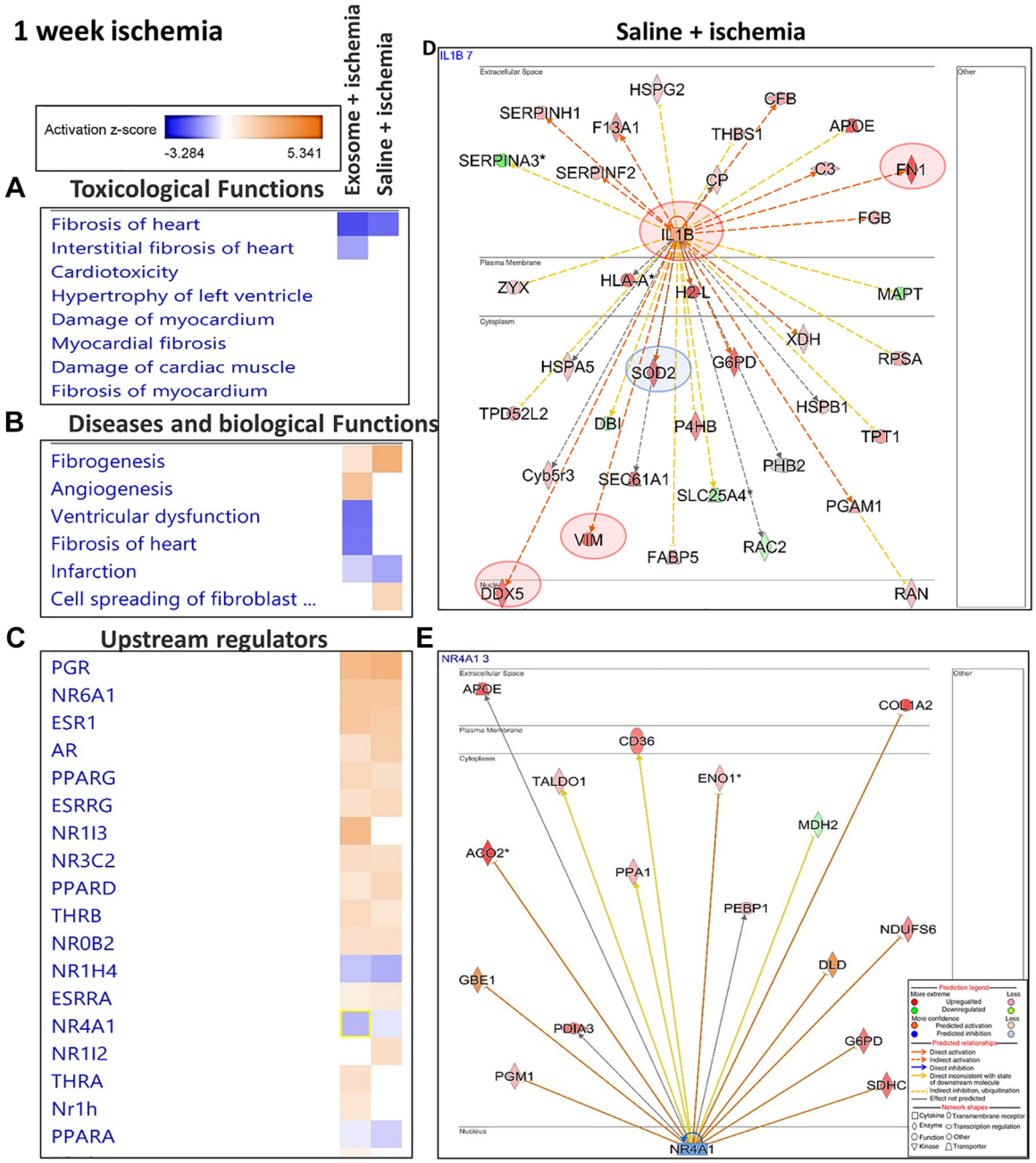

Figure 7. Proteomic analysis of fibrotic events. IPA (QIAGEN, Inc., https://www.qiagenbioinformatics.com/products/ingenuity-pathway-analysis) (33) network analysis revealed toxicological functions in the ischemic hearts which are differentially regulated by MSC exosome treatment signaling networks leading to suppression of fibrosis of heart and interstitial fibrosis of heart (*A*). Although fibrogenesis is increased in ischemic hearts, MSC exosome treatment suppresses the process along with suppression of ventricular dysfunction and stimulating angiogenesis (*B*). Among the differentially regulated upstream regulators, NR4A1 that negatively regulates collagen-1 expression is observed to be suppressed (*C* and *E*). IL-1β appears to be the main culprit in driving the inflammatory cytokine-mediated fibrotic events (*D*). Prediction legend describes the network relationships between different molecules. IPA, ingenuity pathway analysis; MSC, mesenchymal stem cell.

compensatory response to the proinflammatory factors from the infarct areas.

Attempts have been made to exploit stem cells to improve cardiac function following ischemic injury to the heart with the hope that stem cells will facilitate regeneration and/or repair the cardiac muscle and improve cardiac function (45–48). Results of these studies have so far shown some degree of success, with a modest 3%–8% increase in left ventricular ejection fraction and a small 3%–12% decrease in infarct size (49–51). A major limitation of these studies is the assumption that stem cells will transform into cardiomyocytes and replace the damaged or dead cardiac cells, thereby limiting fibrosis. We postulate that stem cells react unfavorably to the toxic inflammatory tissue microenvironment and are unable to adapt and transform into the cardiomyocyte phenotype. We thus focused on using the stem cell exosomes in lieu of stem cells to try to protect the damaged cardiac microenvironment.

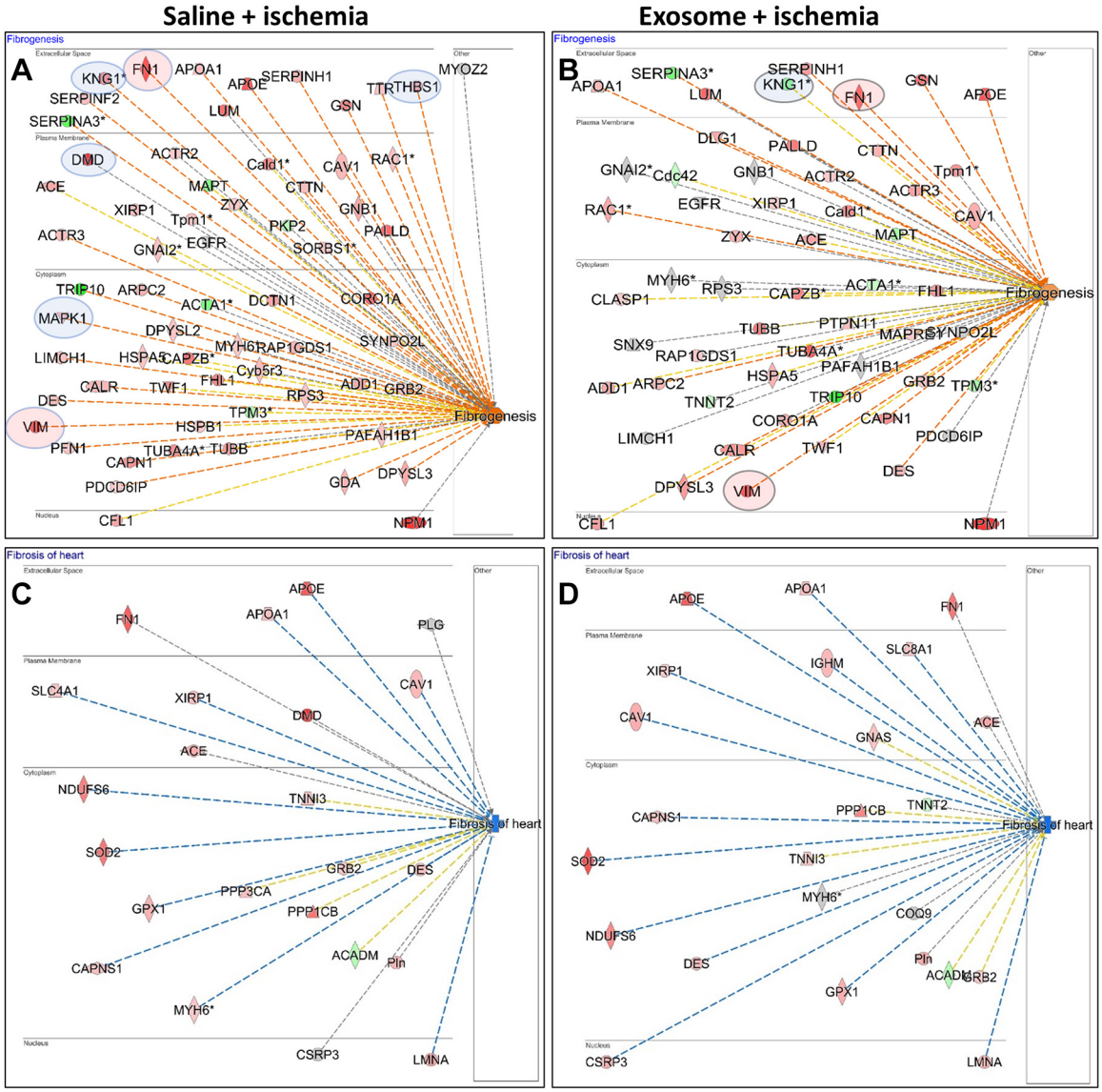

Figure 8. MS analysis of fibrogenesis and fibrosis events in hearts. Although saline-treated ischemic hearts showed an increase in proteins regulating fibrogenesis (*A*) and fibrosis of heart (*C*), MSC exosome treatment suppressed these pathways (*B* and *D*). Prediction legend describes the network relationships between different molecules. MSC, mesenchymal stem cell.

Our previous studies have showed that MSC exosomes afford significant cardioprotection by reducing infarct size, rescuing cardiac function, and retaining ventricular thickness while simultaneously suppressing inflammatory mediators (22). We now present data showing that administration of MSC exosomes, before induction of ischemia, protects the heart against profibrotic ECM remodeling, differentially, in both infarct and peri-infarct areas. Indeed, our study shows that MSC exosomes significantly decrease the expression of inflammatory mediators in both infarct and peri-infarct areas of the ischemic hearts (Figs. 5 and 6). MSC exosomes also suppress profibrotic remodeling and transformation of fibroblasts into myofibroblasts as evidenced by the decrease in vimentin and α-SMA followed by fibronectin levels in the MSC exosome-treated animals (Figs. 5 and 6). Concurrently, there is an increase in MMP2, MMP9, and TIMP2 levels in ischemic hearts with MSC exosome treatment, particularly in the infarct areas. Although, we cannot readily explain the differential changes in vimentin and collagens with MSC exosome, these alterations resulted in a reduction in the scar area along with reduced interstitial fibrosis (Fig. 4).

The fibrotic signaling pathways are driven by the translocation of NF-κB to the nucleus (52, 53). We suggest that MSC exosomes suppressed the activation of proinflammatory p38-MAPK, which in turn inhibited phosphorylation of NF-κB and transcription of its target genes (Figs. 5 and 6).

To understand the changes in the heart, we studied the proteome of different areas of the hearts from saline-treated and exosome-treated mice subjected to LCA ligation. First, we identified profound changes in the signals leading to fibrosis (especially interstitial), fibrogenesis following ischemia (Fig. 7, *A* and *B*).

Interestingly, transcription factors in heart tissues were also differentially regulated (Fig. 7*C*). Among those is the

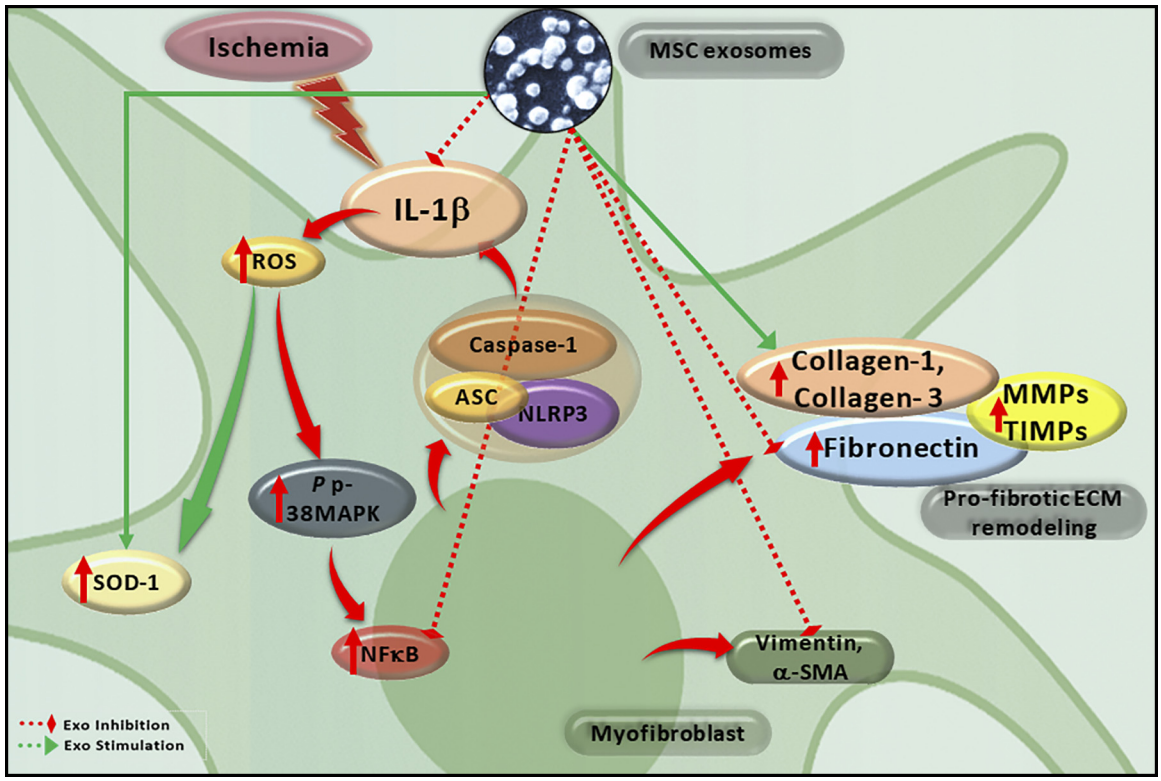

Figure 9. Summary of suppression of fibrotic events with MSC exosome treatment. MSC exosomes provide cardioprotection against inflammation and subsequent fibrotic events. Ischemia stimulates oxidative stress, which activates p-38MAPK, leading to translocation of NF-κB into the nucleus. Activation of NF-κB also leads to increase in fibronectin and collagen-1 and -3 levels precipitating fibrotic scar formation. There is an increase in interstitial fibrosis. MSC exosomes modulate the effects of ischemia by suppressing activation of p-38MAPK and NF-κB, leading to suppression of IL-1β, and inflammasome proteins—NLRP3 and ASC. Fibronectin levels are suppressed, whereas collagen-1 and -3 levels are increased, which helps in maintaining the integrity of damaged heart tissues and providing protection against ventricular dysfunction. ECM, extracellular matrix; MMPs, matrix metalloproteinases; MSC, mesenchymal stem cell; ROS, reactive oxygen species; SOD1, superoxide dismutase 1; TIMPs, tissue inhibitor of metalloproteinases; α-SMA, smooth muscle actin-α.

nuclear receptor NR4A1 (Fig. 8*E*), which, depending on the coregulators and its posttranslational modifications, can function either as a transcriptional activator or repressor (54). NR4A1 has been implicated in macrophage pathophysiology (55, 56). NR4A1 is also implicated in fibroblast physiology where its deletion resulted in increased collagen deposition (57). These data support our findings on collagen levels observed in ischemic hearts (Figs. 5 and 6). Importantly, as we had expected and has been previously extensively reported, IL-1β was found to be the major signal, which probably led to fibrotic events (Fig. 7*D*), and MSC exosomes suppressed IL-1β (Figs. 5 and 6). Further comparison of pathways involving fibrogenesis and fibrosis revealed differential modulation of proteins in MSC exosome-treated hearts that negatively modulated fibrogenesis and suppressed scar formation in the heart (Fig. 8, *A–D*).

In concert with our previous report on proteomics (26), we believe that the cytoprotective protein cargo carried by the exosomes is directly used by the recipient cells. We have also shown that MSC exosomes carry a variety of transcription factors (26) which can potentially be responsible for initiating and triggering anti-inflammatory response in the ischemic mice hearts. These studies are of significant interest because the infarct is well established at 1-wk post-LCA ligation in mice hearts and that cardiac remodeling is already underway, which leads to cardiac dysfunction. Thus, treatment of mice with MSC exosomes increased the heart's ability to induce pro-reparative ECM remodeling (Fig. 9).

To our knowledge, these are the first set of studies showing a link between MSC exosome treatment and suppression of fibroblast mediated profibrotic remodeling. Based on our previous reports (26, 28), it is our conviction that use of exosomes from MSCs would positively modulate the ischemic microenvironment of cardiac tissues and help fibroblasts switch from profibrotic to reparative remodeling of the ischemic ECM. The results of our study lay the groundwork to use MSC exosomes in modulating fibroblast migration and secretory functions.

Study Limitations

There are several limitations of this study. First, after the acute ischemic event, circulating monocytes are recruited to the infarct hearts, and given the scope of our present study, we have not presented the effect of MSC exosomes on the role of recruited and resident macrophages in their inflammatory response. This will be the subject of next communication. Second, we focused our investigation on the early molecular events determining fibrosis in cardiac tissue. We pretreated mice with MSC exosomes 30 min before inducing cardiac ischemia to allow for MSC exosomes to be distributed

and to study the effect of these exosomes as proof of concept. Our observations showed that a single dose of MSC exosomes was sufficient to offer significant cardioprotection and suppress fibrosis over a period of 7 days postischemia. We are now following up by extending our studies on ischemic mice hearts up to 4 and 8 wk. We also are investigating the effects of administration of MSC exosomes after inducing an ischemic event. Third, our proteomic analysis focused on proteins related to inflammation and fibrosis pathways, and processes such as cytokine signaling, ATP production in mitochondria, mitochondrial membrane integrity, etc., that determine the health of cardiomyocytes in diseased hearts were not studied. Fourth, the animal studies were nonblinded. We acknowledge that the lack of blinding is a concern but our MS data corroborates the molecular biology analysis of heart samples. Finally, most of the antifibrotic events can be attributed to global MSC proteomic cargo. We, at this point, have no clear idea of which proteins among that cargo is responsible for the cardioprotective functions. Nonetheless, the early events are important in understanding protein signals, which regulate fibrotic events following ischemic insult to the heart.

Perspectives and Significance

Myocardial ischemia is followed by inflammation and oxidative stress, which leads to the development of fibrosis. It is critical to limit the profibrotic remodeling and activate the reparative remodeling to limit cardiac dysfunction. Here, we show that fibrotic signals in the ischemic heart can be suppressed by treatment of mice with MSC exosomes before LCA ligation. We believe that this is the first report on the early molecular events deciphering the molecular and proteomics events to explain MSC exosome-mediated suppression of scar formation in the ischemic mouse hearts.

SUPPLEMENTAL DATA

Supplemental Fig. S1: https://doi.org/10.6084/m9.figshare.14550978.

GRANTS

This study was supported by Grant-in-Aid from the Department of Veterans Affairs, Veterans Health Administration, Office of Research and Development, Biomedical Laboratory Research and Development, Washington, DC. Additional support was provided by Stebbins Chair in Cardiology funds to J.L.M.

DISCLOSURES

No conflicts of interest, financial or otherwise, are declared by the authors.

AUTHOR CONTRIBUTIONS

R.A.K. and J.L.M. conceived and designed research; R.A.K., X.W., J.C.H., Z.D., and A.J.-P. performed experiments; R.A.K., X.W., J.C.H., Z.D., and A.J.-P. analyzed data; R.A.K., X.W., Z.D., and J.L.M. interpreted results of experiments; R.A.K. prepared figures; R.A.K. drafted manuscript; R.A.K., Z.D., and J.L.M. edited and revised manuscript; R.A.K. and J.L.M. approved final version of manuscript.

ENDNOTE

At the request of the authors, readers are herein alerted to the fact that the authors have posted the proteins and original Western blots at https://doi.org/10.6084/m9.figshare.14550978. These materials are not a part of this manuscript and have not undergone peer review by the American Physiological Society (APS). APS and the journal editors take no responsibility for these materials, for the website address, or for any links to or from it.

REFERENCES

1. **Camelliti P**, **Borg TK**, **Kohl P.** Structural and functional characterisation of cardiac fibroblasts. *Cardiovasc Res* 65: 40–51, 2005. doi:10.1016/j.cardiores.2004.08.020.
2. **Daseke MJ 2nd**, **Tenkorang MAA**, **Chalise U**, **Konfrst SR**, **Lindsey ML.** Cardiac fibroblast activation during myocardial infarction wound healing: fibroblast polarization after MI. *Matrix Biol* 91–92: 109–116, 2020. doi:10.1016/j.matbio.2020.03.010.
3. **Manso AM**, **Kang SM**, **Ross RS.** Integrins, focal adhesions, and cardiac fibroblasts. *J Investig Med* 57: 856–860, 2009. doi:10.2310/JIM.0b013e3181c5e61f.
4. **Shinde AV**, **Frangogiannis NG.** Fibroblasts in myocardial infarction: a role in inflammation and repair. *J Mol Cell Cardiol* 70: 74–82, 2014. doi:10.1016/j.yjmcc.2013.11.015.
5. **Azevedo PS**, **Polegato BF**, **Minicucci MF**, **Paiva SA**, **Zornoff LA.** Cardiac remodeling: concepts, clinical impact, pathophysiological mechanisms and pharmacologic treatment. *Arq Bras Cardiol* 106: 62–69, 2016. doi:10.5935/abc.20160005.
6. **Le Bras A.** Dynamics of fibroblast activation in the infarcted heart. *Nat Rev Cardiol* 15: 379, 2018. doi:10.1038/s41569-018-0025-9.
7. **Ma Y**, **Iyer RP**, **Jung M**, **Czubryt MP**, **Lindsey ML.** Cardiac fibroblast activation post-myocardial infarction: current knowledge gaps. *Trends Pharmacol Sci* 38: 448–458, 2017. doi:10.1016/j.tips.2017.03.001.
8. **Ali SR**, **Ranjbarvaziri S**, **Talkhabi M**, **Zhao P**, **Subat A**, **Hojjat A**, **Kamran P**, **Müller AM**, **Volz KS**, **Tang Z**, **Red-Horse K**, **Ardehali R.** Developmental heterogeneity of cardiac fibroblasts does not predict pathological proliferation and activation. *Circ Res* 115: 625–635, 2014. doi:10.1161/CIRCRESAHA.115.303794.
9. **Nagaraju CK**, **Dries E**, **Popovic N**, **Singh AA**, **Haemers P**, **Roderick HL**, **Claus P**, **Sipido KR**, **Driesen RB.** Global fibroblast activation throughout the left ventricle but localized fibrosis after myocardial infarction. *Sci Rep* 7: 10801, 2017. doi:10.1038/s41598-017-09790-1.
10. **van den Borne SW**, **Diez J**, **Blankesteijn WM**, **Verjans J**, **Hofstra L**, **Narula J.** Myocardial remodeling after infarction: the role of myofibroblasts. *Nat Rev Cardiol* 7: 30–37, 2010. doi:10.1038/nrcardio.2009.199.
11. **Wynn TA.** Cellular and molecular mechanisms of fibrosis. *J Pathol* 214: 199–210, 2008. doi:10.1002/path.2277.
12. **Horn MA**, **Trafford AW.** Aging and the cardiac collagen matrix: novel mediators of fibrotic remodelling. *J Mol Cell Cardiol* 93: 175–185, 2016. doi:10.1016/j.yjmcc.2015.11.005.
13. **Pereira M**, **Rybarczyk BJ**, **Odrljin TM**, **Hocking DC**, **Sottile J**, **Simpson-Haidaris PJ.** The incorporation of fibrinogen into extracellular matrix is dependent on active assembly of a fibronectin matrix. *J Cell Sci* 115: 609–617, 2002.
14. **Sabatier L**, **Chen D**, **Fagotto-Kaufmann C**, **Hubmacher D**, **McKee MD**, **Annis DS**, **Mosher DF**, **Reinhardt DP.** Fibrillin assembly requires fibronectin. *Mol Biol Cell* 20: 846–858, 2009. doi:10.1091/mbc.e08-08-0830.
15. **Sottile J**, **Hocking DC.** Fibronectin polymerization regulates the composition and stability of extracellular matrix fibrils and cell-matrix adhesions. *Mol Biol Cell* 13: 3546–3559, 2002. doi:10.1091/mbc.e02-01-0048.
16. **Valiente-Alandi I**, **Potter SJ**, **Salvador AM**, **Schafer AE**, **Schips T**, **Carrillo-Salinas F**, **Gibson AM**, **Nieman ML**, **Perkins C**, **Sargent MA**, **Huo J**, **Lorenz JN**, **DeFalco T**, **Molkentin JD**, **Alcaide P**, **Blaxall BC.** Inhibiting fibronectin attenuates fibrosis and improves cardiac function in a model of heart failure. *Circulation* 138: 1236–1252, 2018. doi:10.1161/CIRCULATIONAHA.118.034609.

17. **Adamiak M**, **Sahoo S.** Exosomes in myocardial repair: advances and challenges in the development of next-generation therapeutics. *Mol Ther* 26: 1635–1643, 2018. doi:10.1016/j.ymthe.2018.04.024.
18. **Bagno L**, **Hatzistergos KE**, **Balkan W**, **Hare JM.** Mesenchymal stem cell-based therapy for cardiovascular disease: progress and challenges. *Mol Ther* 26: 1610–1623, 2018. doi:10.1016/j.ymthe.2018.05.009.
19. **Garikipati VNS**, **Shoja-Taheri F**, **Davis ME**, **Kishore R.** Extracellular vesicles and the application of system biology and computational modeling in cardiac repair. *Circ Res* 123: 188–204, 2018. doi:10.1161/CIRCRESAHA.117.311215.
20. **Gartz M**, **Strande JL.** Examining the paracrine effects of exosomes in cardiovascular disease and repair. *J Am Heart Assoc* 7: e007954, 2018. doi:10.1161/JAHA.117.007954.
21. **Yuan Y**, **Du W**, **Liu J**, **Ma W**, **Zhang L**, **Du Z**, **Cai B.** Stem cell-derived exosome in cardiovascular diseases: macro roles of micro particles. *Front Pharmacol* 9: 547, 2018. doi:10.3389/fphar.2018.00547.
22. **Kore RA**, **Wang X**, **Ding Z**, **Griffin RJ**, **Tackett AJ**, **Mehta JL.** MSC exosome-mediated cardioprotection in ischemic mouse heart comparative proteomics of infarct and peri-infarct areas. *Mol Cell Biochem* 476: 1691–1704, 2021. doi:10.1007/s11010-020-04029-6.
23. **Mehdi SJ**, **Johnson SK**, **Epstein J**, **Zangari M**, **Qu P**, **Hoering A**, **van Rhee F**, **Schinke C**, **Thanendrarajan S**, **Barlogie B**, **Davies FE**, **Morgan GJ**, **Yaccoby S.** Mesenchymal stem cells gene signature in high-risk myeloma bone marrow linked to suppression of distinct IGFBP2-expressing small adipocytes. *Br J Haematol* 184: 578–593, 2019. doi:10.1111/bjh.15669.
24. **Yaccoby S**, **Wezeman MJ**, **Zangari M**, **Walker R**, **Cottler-Fox M**, **Gaddy D**, **Ling W**, **Saha R**, **Barlogie B**, **Tricot G**, **Epstein J.** Inhibitory effects of osteoblasts and increased bone formation on myeloma in novel culture systems and a myelomatous mouse model. *Haematologica* 91: 192–199, 2006.
25. **Zhan F**, **Huang Y**, **Colla S**, **Stewart JP**, **Hanamura I**, **Gupta S**, **Epstein J**, **Yaccoby S**, **Sawyer J**, **Burington B**, **Anaissie E**, **Hollmig K**, **Pineda-Roman M**, **Tricot G**, **van Rhee F**, **Walker R**, **Zangari M**, **Crowley J**, **Barlogie B**, **Shaughnessy JD Jr.** The molecular classification of multiple myeloma**.** *Blood* 108: 2020–2028, 2006. doi:10.1182/blood-2005-11-013458.
26. **Kore RA**, **Henson JC**, **Hamzah RN**, **Griffin RJ**, **Tackett AJ**, **Ding Z**, **Mehta JL.** Molecular events in MSC exosome mediated cytoprotection in cardiomyocytes. *Sci Rep* 9: 19276, 2019. doi:10.1038/s41598-019-55694-7.
27. **Kore RA**, **Abraham EC.** Inflammatory cytokines, interleukin-1 beta and tumor necrosis factor-alpha, upregulated in glioblastoma multiforme, raise the levels of CRYAB in exosomes secreted by U373 glioma cells. *Biochem Biophys Res Commun* 453: 326–331, 2014. doi:10.1016/j.bbrc.2014.09.068.
28. **Kore RA**, **Edmondson JL**, **Jenkins SV**, **Jamshidi-Parsian A**, **Dings RPM**, **Reyna NS**, **Griffin RJ.** Hypoxia-derived exosomes induce putative altered pathways in biosynthesis and ion regulatory channels in glioblastoma cells. *Biochem Biophys Rep* 14: 104–113, 2018. doi:10.1016/j.bbrep.2018.03.008.
29. **Ding Z**, **Wang X**, **Liu S**, **Shahanawaz J**, **Theus S**, **Fan Y**, **Deng X**, **Zhou S**, **Mehta JL.** PCSK9 expression in the ischemic heart and its relationship to infarct size, cardiac function and development of autophagy. *Cardiovasc Res* 114: 1738–1751, 2018. doi:10.1093/cvr/cvy128.
30. **Wang X**, **Guo Z**, **Ding Z**, **Mehta JL.** Inflammation, autophagy, and apoptosis after myocardial infarction. *J Am Heart Assoc* 7: e008024, 2018. doi:10.1161/JAHA.117.008024.
31. **Lai RC**, **Arslan F**, **Lee MM**, **Sze NS**, **Choo A**, **Chen TS**, **Salto-Tellez M**, **Timmers L**, **Lee CN**, **El Oakley RM**, **Pasterkamp G**, **de Kleijn DP**, **Lim SK.** Exosome secreted by MSC reduces myocardial ischemia/reperfusion injury. *Stem Cell Res* 4: 214–222, 2010. doi:10.1016/j.scr.2009.12.003.
32. **Arslan F**, **Lai RC**, **Smeets MB**, **Akeroyd L**, **Choo A**, **Aguor EN**, **Timmers L**, **van Rijen HV**, **Doevendans PA**, **Pasterkamp G**, **Lim SK**, **de Kleijn DP.** Mesenchymal stem cell-derived exosomes increase ATP levels, decrease oxidative stress and activate PI3K/Akt pathway to enhance myocardial viability and prevent adverse remodeling after myocardial ischemia/reperfusion injury. *Stem Cell Res* 10: 301–312, 2013. doi:10.1016/j.scr.2013.01.002.
33. **Krämer A**, **Green J**, **Pollard J Jr**, **Tugendreich S.** Causal analysis approaches in ingenuity pathway analysis. *Bioinformatics* 30: 523–530, 2014. doi:10.1093/bioinformatics/btt703.
34. **Hwang J**, **Jin J**, **Jeon S**, **Moon SH**, **Park MY**, **Yum DY**, **Kim JH**, **Kang JE**, **Park MH**, **Kim EJ**, **Pan JG**, **Kwon O**, **Oh GT.** SOD1 suppresses pro-inflammatory immune responses by protecting against oxidative stress in colitis. *Redox Biol* 37: 101760, 2020. doi:10.1016/j.redox.2020.101760.
35. **Younus H.** Therapeutic potentials of superoxide dismutase. *Int J Health Sci (Qassim)* 12: 88–93, 2018.
36. **Palumbo-Zerr K**, **Zerr P**, **Distler A**, **Fliehr J**, **Mancuso R**, **Huang J**, **Mielenz D**, **Tomcik M**, **Fürnrohr BG**, **Scholtysek C**, **Dees C**, **Beyer C**, **Krönke G**, **Metzger D**, **Distler O**, **Schett G**, **Distler JH.** Orphan nuclear receptor NR4A1 regulates transforming growth factor-β signaling and fibrosis. *Nat Med* 21: 150–158, 2015. doi:10.1038/nm.3777.
37. **Zeng X**, **Yue Z**, **Gao Y**, **Jiang G**, **Zeng F**, **Shao Y**, **Huang J**, **Yin M**, **Li Y.** NR4A1 is involved in fibrogenesis in ovarian endometriosis. *Cell Physiol Biochem* 46: 1078–1090, 2018. doi:10.1159/000488838.
38. **Chen K**, **Chen J**, **Li D**, **Zhang X**, **Mehta JL.** Angiotensin II regulation of collagen type I expression in cardiac fibroblasts: modulation by PPAR-gamma ligand pioglitazone. *Hypertension* 44: 655–661, 2004. doi:10.1161/01.HYP.0000144400.49062.6b.
39. **Ding Z**, **Liu S**, **Wang X**, **Dai Y**, **Khaidakov M**, **Deng X**, **Fan Y**, **Xiang D**, **Mehta JL.** LOX-1, mtDNA damage, and NLRP3 inflammasome activation in macrophages: implications in atherogenesis. *Cardiovasc Res* 103: 619–628, 2014. doi:10.1093/cvr/cvu114.
40. **Ding Z**, **Wang X**, **Liu S**, **Zhou S**, **Kore RA**, **Mu S**, **Deng X**, **Fan Y**, **Mehta JL.** NLRP3 inflammasome via IL-1β regulates PCSK9 secretion. *Theranostics* 10: 7100–7110, 2020. doi:10.7150/thno.45939.
41. **Hu C**, **Chen J**, **Dandapat A**, **Fujita Y**, **Inoue N**, **Kawase Y**, **Jishage K**, **Suzuki H**, **Li D**, **Hermonat PL**, **Sawamura T**, **Mehta JL.** LOX-1 abrogation reduces myocardial ischemia-reperfusion injury in mice. *J Mol Cell Cardiol* 44: 76–83, 2008. doi:10.1016/j.yjmcc.2007.10.009.
42. **Liu D**, **Zeng X**, **Li X**, **Mehta JL**, **Wang X.** Role of NLRP3 inflammasome in the pathogenesis of cardiovascular diseases. *Basic Res Cardiol* 113: 5, 2018. doi:10.1007/s00395-017-0663-9.
43. **Forrester SJ**, **Kikuchi DS**, **Hernandes MS**, **Xu Q**, **Griendling KK.** Reactive oxygen species in metabolic and inflammatory signaling. *Circ Res* 122: 877–902, 2018. doi:10.1161/CIRCRESAHA.117.311401.
44. **Mittal M**, **Siddiqui MR**, **Tran K**, **Reddy SP**, **Malik AB.** Reactive oxygen species in inflammation and tissue injury. *Antioxid Redox Signal* 20: 1126–1167, 2014. doi:10.1089/ars.2012.5149.
45. **Giri TK**, **Alexander A**, **Agrawal M**, **Saraf S**, **Saraf S**, **Ajazuddin .** Current status of stem cell therapies in tissue repair and regeneration. *Curr Stem Cell Res Ther* 14: 117–126, 2018. doi:10.2174/1574888X13666180502103831.
46. **Menasche P.** Cell therapy trials for heart regeneration - lessons learned and future directions. *Nat Rev Cardiol* 15: 659–671, 2018. doi:10.1038/s41569-018-0013-0.
47. **Tang J**, **Su T**, **Huang K**, **Dinh PU**, **Wang Z**, **Vandergriff A**, **Hensley MT**, **Cores J**, **Allen T**, **Li T**, **Sproul E**, **Mihalko E**, **Lobo LJ**, **Ruterbories L**, **Lynch A**, **Brown A**, **Caranasos TG**, **Shen D**, **Stouffer GA**, **Gu Z**, **Zhang J**, **Cheng K.** Targeted repair of heart injury by stem cells fused with platelet nanovesicles. *Nat Biomed Eng* 2: 17–26, 2018. doi:10.1038/s41551-017-0182-x.
48. **Tompkins BA**, **Balkan W**, **Winkler J**, **Gyongyosi M**, **Goliasch G**, **Fernandez-Aviles F**, **Hare JM.** Preclinical studies of stem cell therapy for heart disease. *Circ Res* 122: 1006–1020, 2018. doi:10.1161/CIRCRESAHA.117.312486.
49. **Kim SH**, **Cho JH**, **Lee YH**, **Lee JH**, **Kim SS**, **Kim MY**, **Lee MG**, **Kang WY**, **Lee KS**, **Ahn YK**, **Jeong MH**, **Kim HS.** Improvement in left ventricular function with intracoronary mesenchymal stem cell therapy in a patient with anterior wall ST-segment elevation myocardial infarction. *Cardiovasc Drugs Ther* 32: 329–338, 2018. doi:10.1007/s10557-018-6804-z.
50. **Laguna G**, **DI Stefano S**, **Maroto L**, **Fulquet E**, **Echevarría JR**, **Revilla A**, **Urueña N**, **Sevilla T**, **Arnold R**, **Ramos B**, **Gutiérrez H**, **Serrador A**, **San Román JA.** Effect of direct intramyocardial autologous stem cell grafting in the sub-acute phase after myocardial infarction. *J Cardiovasc Surg (Torino)* 59: 259–267, 2018. doi:10.23736/S0021-9509.17.10126-6.
51. **Lang CI**, **Wolfien M**, **Langenbach A**, **Muller P**, **Wolkenhauer O**, **Yavari A**, **Ince H**, **Steinhoff G**, **Krause BJ**, **David R**, **Glass ä.** Cardiac cell therapies for the treatment of acute myocardial infarction: a

meta-analysis from mouse studies. *Cell Physiol Biochem* 42: 254–268, 2017. doi:10.1159/000477324.

52. **Dong J**, **Ma Q.** In vivo activation and pro-fibrotic function of NF-κB in fibroblastic cells during pulmonary inflammation and fibrosis induced by carbon nanotubes. *Front Pharmacol* 10: 1140, 2019. doi:10.3389/fphar.2019.01140.
53. **Luedde T**, **Schwabe RF.** NF-κB in the liver–linking injury, fibrosis and hepatocellular carcinoma. *Nat Rev Gastroenterol Hepatol* 8: 108–118, 2011. doi:10.1038/nrgastro.2010.213.
54. **Kurakula K**, **Koenis DS**, **van Tiel CM**, **de Vries CJ.** NR4A nuclear receptors are orphans but not lonesome. *Biochim Biophys Acta* 1843: 2543–2555, 2014. doi:10.1016/j.bbamcr.2014.06.010.
55. **Hamers AAJ**, **Vos M**, **Rassam F**, **Marinković G**, **Marincovic G**, **Kurakula K**, **van Gorp PJ**, **de Winther MPJ**, **Gijbels MJJ**, **de Waard V**, **de Vries CJM.** Bone marrow-specific deficiency of nuclear receptor Nur77 enhances atherosclerosis. *Circ Res* 110: 428–438, 2012 [Erratum in *Circ Res* 110: e46, 2012]. doi:10.1161/CIRCRESAHA.111.260760.
56. **Hanna RN**, **Shaked I**, **Hubbeling HG**, **Punt JA**, **Wu R**, **Herrley E**, **Zaugg C**, **Pei H**, **Geissmann F**, **Ley K**, **Hedrick CC.** NR4A1 (Nur77) deletion polarizes macrophages toward an inflammatory phenotype and increases atherosclerosis. *Circ Res* 110: 416–427, 2012. doi:10.1161/CIRCRESAHA.111.253377.
57. **Wong W.** Limiting TGF-β signaling to prevent fibrosis. *Sci Signal* 8: ec34, 2015. doi:10.1126/scisignal.aaa9108.